A-9 Nonlinear Optics

From Physics 191r

Revision as of 15:39, 23 April 2010 by Peidle (Talk | contribs | block)
(diff) ← Older revision | Current revision (diff) | Newer revision → (diff)

NONLINEAR OPTICS AND LASER SPECTROSCOPY

author: Mikhail Lukin (2003)

first experiment: II

Contents

- 1 Introduction
- 2 Background
- 3 Atomic saturation
- 4 Saturation spectroscopy
- 5 Two-photon transitions and dark resonances
- 6 Nonlinear polarization spectroscopy
- 7 Suggested experiments
  - 7.1 Laser spectroscopy of Rb:
  - 7.2 Note for diode laser operation:
  - 7.3 Doppler-free saturation spectroscopy:
  - 7.4 Nonlinear polarization spectroscopy:
- 8 Measurement of slow pulse propagation
- 9 APPARATUS
  - 9.1 Laser
  - 9.2 Rubidium Vapor Cells
  - 9.3 Wave Plates and Polarizers
    - 9.3.1 Quarter Wave Plate
    - 9.3.2 Half Wave Plate
    - 9.3.3 Linear Polarizer
    - 9.3.4 Polarizing Cubes
  - 9.4 Pockels Cell
  - 9.5 Photodetectors
  - 9.6 Magnetic Shield, Oven and Solenoid
    - 9.6.1 Magnetic Shield
    - 9.6.2 Oven
  - 9.7 Solenoid
- 10 NOTES
- 11 REFERENCES
- 12 BENCH NOTES
- 13 APPENDIX: Alternate Perspective on Dark Resonance

Introduction

In this experiment several techniques from modern nonlinear optical physics and laser spectroscopy are investigated. The experiment utilizes a highly coherent source of light, provided by an extended cavity diode laser, to probe the spectroscopic properties of atomic Rubidium vapor, as well as novel coherent phenomena that arise from the interaction of light and atoms. Proposed experiments include:

- a) observation and identification of Rb absorption lines
- b) investigation of sub-Doppler resonances in a standing-wave laser field
- c) investigation of the absorptive and dispersive properties of "dark-resonances" through measurement of non-linear polarization

phenomena such as the Faraday effect and
- d) measurement of ultra-slow group velocities for light pulses, which are associated with narrow dark-resonances.

Background

Whenever a light beam interacts with atoms, the amplitude and phase of the light can be modified. For example, amplitude changes are caused by light absorption, in which energy is transfered from the light beam to the atoms and then subsequently reemitted as fluorescence. Phase shifts are associated with the refractive properties of the atomic medium, which are conventionally described by the index of refraction n.

Associated with the refractive properties of materials is the modification of the speed at which light propagates. In practice, several different speeds (i.e., velocities) of light are important and should be distinguished. The "phase velocity" is the speed of planes of light with constant phase. For a given frequency ω and wavenumber k, the phase velocity is defined as $v = \omega/k \equiv c/n$, where c is the famous "speed of light", i.e., the phase velocity of light in a vacuum (where $n = 1$). In cases where n depends upon the light's frequency or wavenumber, each frequency component of a light pulse travels with its own phase velocity. Thus the speed at which the light pulse envelope travels can differ from the phase velocity. This light pulse speed, known as the "group velocity", is defined as $v_g = \partial\omega/\partial k \equiv c/(n + \omega\partial n/\partial\omega)$.

The strength of the interaction between light and atoms is a function of the wavelength or frequency of light. When the light's frequency matches the frequency of a particular atomic transition, a resonance condition occurs. In this case, the optical response of the medium is greatly enhanced. Light propagation is then accompanied by strong absorption and dispersion [1][2], as the atoms are actively promoted into fluorescing excited states. Such "resonance lines" appear as sharp peaks in atomic absorption and fluorescence, accompanied by steep dispersion of the refractive index.

For strong light-atom interactions, it is also important that the angular momentum difference of the atomic transition (determined both by the properties and relative occupation of the atomic levels) matches the angular momentum carried by the photons (a function of the light's polarization). If there is a complete mismatch between the angular momentum carried by the photons and the properties of the atomic medium, then absorption of the light can be completely shut off -- even exactly at resonance -- because angular momentum cannot be conserved. (Read more about it!)

While discussing resonant phenomena it is often convenient to use the concept of the two (or three) level atom. Whereas in real life any atomic system has a large number of energy levels, only a few resonantly-coupled levels are effectively involved when narrow-band (i.e., narrow spectrum) laser light is used. In fact, most (but not all!) of the physics of near-resonant atom-light interactions can be understood using a theoretical description involving only two atomic levels (Figure 1a). The response of such a system to light can be analyzed by using the standard methods of quantum mechanics[2], or by using a simple classical oscillator model[1]. Figure 1b shows the result of such an anlysis for: (i) the transmission of light through an ensemble of two-level atoms; and (ii) the ensemble's refractive index as a function of the detuning of the light's frequency from resonance, $\Delta = \omega - \omega_0$, where ω_0 is the atomic resonance frequency. Atomic absorption (and hence transmission) of light is typically described by a Lorentzian function, which is symmetric in the detuning Δ; whereas the deviation of the refractive index from unity is described by the derivative of the Lorentzian function with respect to frequency, which is an anti-symmetric function of the detuning (why?).

An important property of an atomic resonance line is its width. Whereas in principle, perfectly isolated atoms can have infinitely sharp lines, there is always a non-zero width in practice.[3] In atomic gases, several important factors contribute to the resonance linewidth for transitions in the infrared and optical regime.

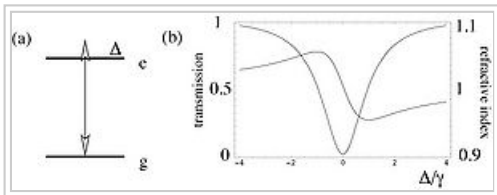

Figure 1. (a) Energy level schematic for a two level atom interacting with a narrow-band light beam. (b) Light transmission and refractive index for a medium made of two-level atoms, as a function of frequency detuning of the light from resonance, $\Delta = \omega - \omega_0$.

One fundamental contributor to the linewidth is the finite lifetime of atomic states, τ_{sp}, associated with spontaneous photon emission due to atomic coupling to vacuum fluctuations. The corresponding linewidth is then $\gamma_{sp} \sim \frac{1}{\tau_{sp}}$, which is about 5 MHz in the case of the commonly-used near-infrared transitions in Rb.

An important mechanism for further broadening of the resonance linewidth is associated with atomic motion in a gas. Due to the Doppler effect, the resonant frequency of an atom moving with velocity $\vec{v}$ is shifted by the amount $\delta\nu = (\vec{k} \cdot \vec{v})$, where $\vec{k}$ is the light's wavevector, assuming the sample size is greater than the light's wavelength. Since a thermal ensemble of atoms has a Maxwellian distribution of velocities with spread Δv_T, the linewidth of an infrared or optical transition will have a characteristic width $\Delta\nu_T \sim k \times \Delta v_T$. The magnitude of this so-called Doppler broadening in Rb is about 500 MHz at room temperature.

These two mechanisms result in fairly broad linewidths in simple optical measurements. However, it is possible to observe much sharper spectral lines if coherent effects that are nonlinear in light power are considered. This is the essence of nonlinear laser spectroscopy.

Atomic saturation

All techniques for high-resolution spectroscopy studied in this advanced lab experiment utilize, in one way or another, a nonlinear response of atoms to light. "Atomic saturation" is a generic signature of effects that are nonlinear in light power. As a rule, such effects appear only when the light power exceeds some threshold value. In practice, however, a variety of different saturation mechanisms can co-exist, each characterized by a different saturation intensity. A textbook example of saturation occurs for two-level atoms and resonant light, and is governed by two competing processes (Figure 2a). On the one hand, the atoms are promoted from the ground state into the excited state by absorbing light. On the other hand, atoms decay back to the ground state by spontaneous emission or are driven back by stimulated emission. Saturation occurs when the rate of optical excitation is on the order of the spontaneous decay rate, γ_r. Then, the ability of the atoms to absorb light drops because the population of the two atomic states becomes equalized. The resonance is thus said to be "saturated".

A different example involves so-called "optical pumping", which takes place in a system with more than two relevant levels (such as that shown in Figure 2b). Here, the two lower levels correspond to, e.g., hyperfine or Zeeman sublevels of the electronic ground state. Optical transitions (involving either laser excitation or spontaneous decay) are allowed between states $|g_1\rangle \rightarrow |e\rangle$ and $|g_2\rangle \rightarrow |e\rangle$. At the same time, relaxation between the two lower states is typically extremely slow (why?). The two optical transitions can be excited selectively by lasers of differing frequencies or polarization. The polarization selectivity is due to selection rules that reflect angular momentum conservation in atom-field interactions.

Optical pumping occurs when only one of the optical transitions, say $|g_1\rangle \rightarrow |e\rangle$, is excited by laser light of a particular frequency or polarization. An excited atom can decay to the ground state via two paths, both via spontaneous emission. It can either make a transition to its original state $|g_1\rangle$ in which case it will be subsequently excited again, or it can decay into the decoupled state $|g_2\rangle$. The atoms in the state $|g_2\rangle$ are no longer excited by light; they can leave this state only slowly via non-radiative relaxation to state $|g_1\rangle$ at the rate γ_0. Hence for sufficiently strong laser light the atoms will be pumped into the decoupled state, and light absorption will disappear. This effect is another example of atomic saturation. However, the laser power required to observe such saturation can be much smaller than in the two-level case. For optical pumping, a significant change in the light absorption will occur when the atomic excitation rate due to the laser is comparable to the non-radiative relaxation rate, γ_0. Typically, $\gamma_0 \ll \gamma_r$, hence the saturation intensity for optical pumping can be very small.

Saturation spectroscopy

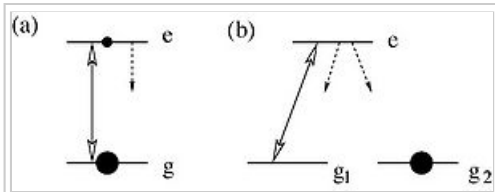

Figure 2. Different atomic saturation mechanisms. (a) Two-level saturation due to the competition between stimulated and spontaneous radiative processes. (b) Optical pumping into a decoupled atomic state in a three-level system.

Atomic saturation is an effective tool for high-resolution laser spectroscopy. A simple example is sub-Doppler resonances, which are associated with the so-called hole-burning phenomenon in standing-wave light fields. In this technique, two counterpropagating, overlapping laser beams of exactly the same frequency interact with an ensemble of two-level atoms. To understand the effect of the light, one can divide the atoms in the ensemble into groups, each of which is characterized by a particular projection of the atomic velocity v_z onto the direction of the laser beam path (Figure 3). When the laser frequency differs by Δ from the resonant frequency of the atoms, ω_0, one beam interacts resonantly with the group of atoms with velocity component $v_z = \Delta/k$ (where k is the light wavenumber), and the other beam interacts with a different group of atoms, those with velocity component $-\Delta/k$. However, when the laser frequency is on resonance with the atoms ($\Delta = 0$), the two beams interact with the same group of atoms, those with velocity component parallel to the beams ≈ 0. Under these circumstances the pair of beams can act together and thus strongly saturate the atoms over a very narrow range of frequencies, which under proper conditions can approach the natural width determined by the spontaneous emission lifetime of the atomic transition. For example, as shown in Figure 3b, a narrow fluorescence dip appears in cases such as optical pumping when atomic saturation results in decreased atom-light interaction.

Two-photon transitions and dark resonances

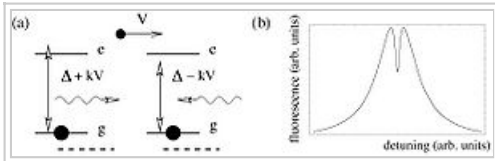

Figure 3. The physics of sub-Doppler resonances in a standing-wave light field. (a) A moving atom experiences laser fields of shifted frequency. The effective detuning is different for the two oppositely-propagating field components. Dashed

Even sharper spectral lines can be obtained by using several light beams of differing frequencies or polarizations, such that absorption or emission of several (e.g., two) photons simultaneously is possible. Such processes can induce transitions between metastable atomic states with long lifetimes and coherence times, and hence can produce very narrow resonances.

To illustrate the physical mechanism behind this effect, consider the three-level atomic system shown in Figure 4a. Here, two metastable states are coupled to a common

sublevels correspond to decoupled states into which the atoms can be optically-pumped. (b) Typical sub-Doppler resonance as seen in a fluorescence dip in a Doppler-broadened sample subject to a standing-wave light field.

excited state by two laser fields. In the situation relevant to our advanced lab experiment, the two lower states correspond to a pair of Zeeman sublevels of Rb, $|g_1\rangle$ and $|g_2\rangle$, which have spin angular momentum $-\hbar$ and $+\hbar$ respectively; and the two fields are represented by two circular polarization components of a single laser beam, with photons that carry angular momentum of $+\hbar$ and $-\hbar$, respectively. The energy level diagram shown in Figure 4b is more realistic because it also shows the Zeeman sublevel with M=0 (i.e., no spin angular momentum). To first approximation, this intervening Zeeman level does not participate in the two-photon transition, and hence can be ignored. Two different frequency detunings are important in this situation. A common "one-photon" detuning, Δ, of the two field components from atomic resonance is controlled by the laser frequency. A so-called "two-photon" detuning, δ, corresponding to a mismatch between the frequency difference of the two laser fields and the separation of the levels $|g_1\rangle$ and $|g_2\rangle$, is most easily controlled by shifting the sublevels with an external magnetic field B_z via the Zeeman effect.

The response of this atomic system to weak laser fields is easy to understand. Atomic absorption will be maximal when the fields are tuned to one-photon resonance and the magnetic field is absent. If the frequency of the light is fixed, then increased two-photon detuning δ can only cause reduced absorption. Note that with a non-zero two-photon detuning, there are different refractive indexes for the two field components, since positive δ corresponds to positive detuning for one field component and negative detuning for the other one; see Figure 4c. As a result, the two field components acquire a relative phase shift proportional to the difference of the refractive indexes, Δn.

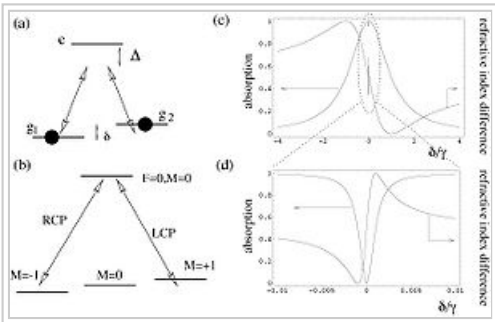

Figure 4. (a) A simplified model for "dark-resonances" and the nonlinear Faraday effect is given by a three-level atomic system and two optical fields. (b) An example realization of the simplified model: a $F = 1 \rightarrow F = 0$ manifold of atomic states and two circular polarization components of a single laser beam; a magnetic field *B* causes Zeeman-shifts of the $M = \pm 1$ levels by $\pm\delta/2 = g\mu_B B_z$. To first approximation, the M=0 level plays no role and can be ignored. (c) Atomic absorption and refractive index difference for the two optical field components as a function of level splitting δ. Note that the width of these linear features is on the order of the Doppler width in our experiment. Here, a fixed tuning of the laser, $\Delta = 0$, is chosen, (d) Narrow features in the absorption and dispersion, corresponding to nonlinear dark-resonances. The linewidth is limited by the relaxation rate of the Zeeman coherence and can be measured in our experiment.

A qualitatively different behavior occurs in the nonlinear, saturated regime. As the intensity of either or both of the two light fields increases, there are no obvious decoupled states for optical pumping. Although saturation similar to that of two-state atom could be expected, this is not what happens in practice. Instead, the atoms remain in the ground states $|g_1\rangle$, $|g_2\rangle$, but they are no longer promoted to the electronic excited state $|e\rangle$: i.e., the atomic medium has become transparent to nominally-resonant light. See Figure 4d. This "electromagnetically induced transparency" (EIT) is an atomic interference effect in which the strong fields drive the atoms into a coherent superposition of the two ground states that is decoupled from the excited state. When the two field components have identical amplitudes and phases, the resulting antisymmetric superposition of states is $1/\sqrt{2}(|g_1\rangle - |g_2\rangle)$. Note in particular that the minus sign corresponds to a specific phase difference (π) between the ground states. Atoms in this superposition state have two possible "absorption" paths (i.e., two components of the transition matrix element): they can begin in either $|g_1\rangle$ or $|g_2\rangle$ and end in the same final state $|e\rangle$. The quantum mechanical amplitudes for such absorption paths can interfere. In particular, when the two transition electric dipoles oscillate out of phase, then the interference is destructive. In this case none of the atoms are promoted to the electronic excited state, leading to vanishing light absorption. This phenomenon is the essence of the so-called "dark resonances".

In order to better understand the origin of dark-resonances and EIT, it is instructive to consider the phenomena in a different basis of states. In the absence of a magnetic field we are free to choose any direction of quantization we want. For example, consider a basis in which the quantization axis is chosen along the direction of the optical field polarization. In this basis (with appropriate reassigning of the quantum numbers describing the states $|g_1\rangle$, $|g_2\rangle$, and $|e\rangle$), selection rules imply that only one optical transition (corresponding to $\Delta M_F = 0$) will be coupled by the light, resulting in the usual optical pumping situation shown in Figure 2b. The decoupled state in this basis exactly corresponds to the "dark" superposition of atomic states discussed above.

Many of the important properties of dark-resonances result from the fragile nature of quantum mechanical interference. The ideal transparency is attained only if the frequency difference between the two field components precisely matches the frequency separation between the two lower states, i.e., in the case of $\delta = 0$. If the matching is not perfect, then the interference is not ideal and the medium becomes absorbing. Thus the transparency spike that appears in the absorption spectrum (as a function of two-photon detuning) is typically very narrow (Figure 4c).[4] The tolerance to frequency mismatch can be increased by using stronger coupling fields, which cause power broadening of the dark-resonance, and hence induce more robust destructive interference.

The refractive properties of a dark-resonance are also remarkable. Since the atoms are decoupled from the light fields in an ideal dark state, the refractive index at resonance is nearly equal to unity. Thus the propagation velocity of a phase front (i.e., the phase velocity) is equal to the speed of light in vacuum, c. However, the narrow transparency resonance is accompanied by a very steep variation of the refractive index as shown in Figure 4c. As a result, the envelope of a light wave-packet (i.e., a light pulse) propagating in the medium moves with a group velocity v_g that is much smaller than c, a phenomenon known as "slow light".

Nonlinear polarization spectroscopy

The ideas outlined above can be probed experimentally in a simple arrangement corresponding to polarization spectroscopy. The polarization of a light beam can be rotated when interacting with an optically active medium placed in a magnetic field. This is the essence of the conventional Faraday effect. As a rule, large magnetic fields are required to produce a sizable rotation angle. For example, in atomic vapor, Zeeman level shifts on the order of the Doppler width (hundreds of MHz) are required to observe the conventional Faraday effect. The situation changes when effects that are nonlinear in light power are considered. Of particular interest is a nonlinear Faraday effect involving an ensemble of atoms with a pair of ground-state Zeeman sublevels (see Figure 4): these allow one to observe extremely narrow dark-resonances and to achieve significant polarization rotation at modest magnetic fields.

To relate polarization spectroscopy to the ideas discussed above, consider the energy level scheme of Figure 4, corresponding to atoms with total angular momentum $F = 1$ in the ground state and $F = 0$ in the excited state. Magnetic quantum numbers $M_F = 0, \pm 1$ distinguish the three Zeeman sublevels of the ground state. Although the three sublevels are degenerate for perfectly isolated atoms, the degeneracy can be lifted, e.g., by applying a static magnetic field along the laser beam propagation path. We will consider propagation of linearly polarized light in such an atomic medium. Let z be the direction of light propagation as well as the angular momentum quantization axis. In this basis, linearly polarized light can be decomposed into two equal-intensity components of circularly polarized light with opposite helicity $\sigma_\pm$: $E = E_+ \hat{\sigma}_+ + E_- \hat{\sigma}_-$. Total angular momentum conservation results in an increase (decrease) of atomic angular momentum by $\hbar$ when a left (right) circularly polarized photon is absorbed. This corresponds to changing the atomic magnetic quantum number by $\Delta M_F = \pm 1$ as diagrammed in the coupling scheme shown in Figure 4. The magnetic field B_z applied along the z axis shifts the energy of states $M_F = \pm 1$ in the opposite direction, due to the Zeeman effect. Hence the situation here is analogous to that considered in a previous section with two-photon detuning $\delta = gB_z$. In the absence of a magnetic field, the two circularly-polarized components drive the atoms (via optical pumping) into a coherent superposition of the ground-state Zeeman sublevels that is decoupled from the light fields: the so-called "dark state". The field B_z applied to such an atomic ensemble causes a splitting of the sublevels, which destroys the dark state, increases absorption of the optical field, and induces phase shifts which are different for right (RCP) and left (LCP) circularly polarized light. Hence, as linearly polarized light passes through the medium, the direction of polarization changes by an angle $\phi = \Delta n k L$ due to the differing changes in the phase of the two circular components. Here L is the length of the sample cell, k is the wavenumber of the incident light, and Δn is the refractive index difference of the atomic medium for RCP and LCP light.

Thus one sees that the absorptive properties of dark-resonances can be measured by monitoring the transmission of a linearly polarized light beam as a function of magnetic field, whereas the dispersive properties can be measured by observing the rotation of the light's polarization.

Some of the applications of narrow dark-resonances include: atomic spectroscopy, high-precision magnetometry, and coherent control of light pulses. All of these effects can be understood quantitatively in the framework of semiclassical atom-field interactions. In this theory, light fields are treated classically using Maxwell's equations, whereas atomic energy levels are considered quantum mechanically. Hence, Schrodinger equations are used for atomic dynamics[2][5][6].

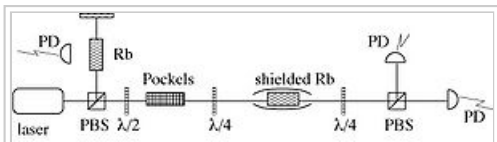

Figure 5. Schematic of the experimental setup. The laser beam passes through a polarizing beam splitter (PBS) and two Rb cells, one magnetically shielded and one unshielded. Transmission of light through the shielded cell and fluorescence from the unshielded cell are detected by two photodiodes (PD). An optional Pockels cell (PC) for time-dependent polarization control of the incident light is also indicated. Additional λ / 2 and λ / 4 waveplates can be used.

Suggested experiments

Laser spectroscopy of Rb:

You should observe the Rb absorption lines both in transmission measurements and fluorescence. Identify each of the lines with a corresponding transition between a pair of hyperfine sublevels of the isotopes ^{87}Rb and ^{85}Rb. What determines the relative strength and shapes of the lines? Use a polarizing beam splitter to split your beam into two parts and align them as shown in Figure 5.

Note for diode laser operation:

This is an expensive piece of equipment and care must be taken to extend its lifetime. Whereas the laser degrades very slowly while operating steadily, the most damage can be done when it is being turned on and off or when large changes occur in the current. For this reason, leave the laser on during the entirety of a lab session that involves its use. While turning the power on and off, do not change the current settings.

Doppler-free saturation spectroscopy:

Using a mirror to retro-reflect the beam back into the absorption cell and thus to create an optical standing-wave, observe and study narrow, sub-Doppler features in fluorescence. Zoom in on each of the transition groups. Determine the atomic transition corresponding to each resonance. Identify also the crossover resonances and explain their origin. Investigate what determines the width of the observed features.

Nonlinear polarization spectroscopy:

The experiment is shown schematically in Figure 5. The laser beam should be collimated to have a diameter of a few mm and should pass through a magnetically shielded vapor cell. The cell should be heated to produce Rb atomic densities in the range of $10^{11} - 10^{12}$ cm^{-3}. (What is the corresponding temperature?) A longitudinal magnetic field is created by a solenoid placed inside the magnetic shields. (What field strength should you use?)

Before starting this experiment you should understand how polarization measurement works. To this end, the following calculation is important. Consider laser light that passes through a linear polarizer and a near-resonant atomic medium (which rotates the light polarization by an angle ϕ and also attenuates the light). The light then passes through another polarizer with an optical axis that is rotated by an angle θ with respect to the first polarizer, and then finally through a photodetector. Calculate the expected signal dependance on ϕ for different orientations of $\theta = 0, 45^\circ, 90^\circ$. For which setting of θ would you expect to see the largest signal in the case of small ϕ?

Equipped with this knowledge, you are now in a position to observe and understand nonlinear Faraday resonances. For the most optimal setting of θ, tune the laser manually across the Rb absorption lines while monitoring the changes in light polarization (using, e.g., two crossed polarizers) as the magnetic field is varied periodically. (What is a convenient frequency for this field variation?) Observe the nonlinear Faraday resonance and study the signal as a function of light intensity, atomic density and laser detuning (i.e., tune the laser to the different hyperfine components). Calibrate your magnetic field scan and estimate the width of the resulting resonances. For the several specific transitions, study the signal dependence on θ, as well as on light power. In addition, observe the dark-resonance effect by monitoring the total transmitted intensity of linearly polarized light through the cell as a function of magnetic field and without a second polarizer (this corresponds to a measurement of absorptive properties).

The following investigations should be pursued:

- a) study the width of the dark-resonance as function of light power
- b) determine the polarization rotation angle from your data sets, and determine the dependence on laser power
- c) from these measurements calculate the absolute change in the refractive index near the dark-resonance as well as the slope of the refractive index, and then estimate the corresponding group velocity
- d) determine the absolute change in the total transmitted intensity across the dark-resonance
- e) explain why Faraday resonances differ so much even for nearby transitions, e.g., for $F = 1 \rightarrow F = 1$ and $F = 1 \rightarrow F = 2$ transitions in Rb.

Measurement of slow pulse propagation

Finally, if the polarization of the incident field is modulated in time (which can be done using a Pockels cell -- how?), it is possible to directly measure delays in the group velocity of a light pulse ("slow light") associated with differential propagation of LCP and RCP components of the light. In this measurement it is more convenient to work with elliptically polarized light consisting of a strong LCP (σ_+) component and a weak, time-varying RCP (σ_-) component. The essential idea is to have a strong component that will make the medium transparent by optical pumping. This component will propagate though the atoms with velocity close to c and will serve as a reference. A pulse of the weaker σ_- component will then experience a large delay associated with the steep variation of the refractive index near the dark-resonance. Making the medium transparent for a weak signal beam by using another strong beam is the essence of Electromagnetically Induced Transparency (EIT).

As a warm-up, develop a theoretical model for the propagation of a continuous, amplitude-modulated light beam through a medium with steep dispersion of the refractive index. Show, in particular, how the difference in the refractive index for different frequency components of the beam results in a delay of the modulated envelope.

Begin the experiment by learning the operation of the Pockels cell. Test its operation by modulating linearly polarized light with a harmonic signal. Proceed by inserting $\lambda/4$ wave plates and orienting them properly such that light in the Rb cell is mostly LCP (σ_+) with only a weak RCP (σ_-) component. With the Pockels cell modulation off, set your detection system such that it can monitor the transmission of the LCP and RCP components independently. Tune the laser close to the transition that has the best Faraday resonances, and repeat the Faraday measurement of the previous section. Observe a narrow resonance in the transmission of the weak RCP field component as a function of magnetic field.

Turn off the magnetic field modulation and instead modulate the input voltage to the Pockels cell. It is best to choose an offset to the Pockels cell voltage such that the modulation depth of the weak RCP component is not too large. (When the modulation depth is 100%, somewhat more complex behavior will be observed if the laser is tuned to resonance. You can also try to observe and explain it!). For a modulation rate on the order of the resonance width you should be able to observe a delay of the modulated signal, which can varied by changing the laser frequency (single-photon resonance condition) or the magnetic field (two-photon resonance). Parameters that can be used to optimize the delay are: light power and atomic density. From the observed delays calculate the group velocity and compare it with the estimates obtained in the previous section.

APPARATUS

Laser

Before turning on the laser, discuss operating procedures and safety precautions with the faculty or staff. The laser is a Class IIIb device. Your vision can be damaged by even a momentary exposure. Never place your eye at the level of the laser beam. Keep all beams confined within the footprint of the optical table. Wear laser safety glasses whenever putting any component into or out of the beam. When using the IR card to view the beam, hold the card at such an angle that the specular reflection will travel downwards.

The light source used in this experiment is a Vortex 6017 tunable external-cavity diode laser, manufactured by New Focus. In a tunable diode laser, the rear facet of the diode crystal together with a diffraction grating and mirror define an external cavity. (See the figure in the laser operating manual, page 49.) Small changes in the position of the mirror make small changes in the length of the cavity, and thus in the wavelength of the light. A piezoelectric transducer (PZT) is used to move the mirror.

The button labeled “Display” on the laser control unit toggles between laser current, laser power, PZT voltage, and an auxiliary function, which is not used. When PZT voltage is selected and the “Set” button is illuminated, one can manually tune the PZT voltage and thus the laser wavelength. The center frequency of the laser is 794.99nm (vacuum). A rear-panel voltage input makes it possible to sweep through a range of wavelengths repeatedly. An input of ±4.5 V sweeps across the entire range of the PZT (approximately 0.25 nm).

The laser control unit includes a temperature controller, which stabilizes the laser diode at about 18˚C. When the key-switch is activated, the temperature controller turns on. Several minutes are needed to achieve stable temperature.

To turn on the laser itself, use the button marked “Power.” When the button is pressed, the laser current ramps up above the lasing threshold.

In order to prolong the life of the laser, minimize cycling the Power. In practice this usually means turning on the beam at the beginning of a lab session and turning it off at the end. The temperature controller (key switch) can be left on for the duration of the experiment. The current setpoint is generally left at the factory-recommended value of 33.1mA. The laser is normally operated in constant current mode as opposed to constant power mode.

Rubidium Vapor Cells

Four rubidium vapor cells are available. Each cell is cylindrical - three inches long and one inch in diameter. The ends are made from optical quality glass. The first cell contains only rubidium vapor; the pressure in the cell is simply the vapor pressure of rubidium at room temperature. Small droplets of solid rubidium are visible on the wall of the cell. This is the cell mounted in the saturated absorption measurement at 90° to the primary beam axis on the optical table.

Three other cells contain a neon buffer gas in addition to rubidium. The cell most likely found already mounted in the magnetic shield contains ^{87}Rb only and 3 Torr of neon. The other two cells contain rubidium in the naturally occurring ratio. The pressure of neon in these cells is 3 Torr and 10 Torr respectively. Any of these cells can be used to observe dark resonance and slow light. The buffer gas minimizes collisions of rubidium atoms with the walls.

Wave Plates and Polarizers

Manipulating the polarization of light is critical in this experiment because selection rules for the atomic transitions are determined by how the polarization of the light is chosen. If you are not completely comfortable with the use of wave plates to create circular and elliptical polarization, take some time to investigate their behavior early on in your work.

It can be useful to look at computer simulations such as http://home3.netcarrier.com/~chan/EM/PROGRAMS/POLARIZATION/ which demonstrates how polarization components add after passing through wave plates.

Light traveling in a medium slows down by a factor of the index of refraction of the medium: $v_n = c/n$. Wave plates are used to preferentially retard the light wave along a certain axis. Wave plates are made of birefringent material i.e., a crystalline material in which the index of refraction which varies with crystal direction. The direction in which the light slows down least is called the “fast axis.”

Quarter Wave Plate

A quarter wave plate retards light polarized along its fast axis by 90° less than it retards light polarized along the perpendicular direction. Consider a quarter wave plate oriented with its fast axis vertical (along the y-axis). Linearly polarized light is incident upon the wave plate. Define θ as the angle between the polarization direction and the positive y-axis.

If $\theta = 45°$, $E_y = E_x$. E_x, however is delayed by one-quarter period. Thus the net electric field vector leaving the plate rotates. The rotation can be either clockwise ($\sigma+$) or counterclockwise ($\sigma-$) as viewed upstream along the propagation direction depending on whether plus or minus 45° is chosen.

If $\theta = 0°$ or $\theta = 90°$, no net relative phase change occurs; the polarization is unaffected. If θ is between 0° and 45°, elliptical polarization results. In the computer simulation, you can create elliptical polarization by choosing a 90° phase difference between E_y and E_x and making the magnitudes different.

Half Wave Plate

As for the quarter wave plate, if the fast axis is parallel or perpendicular to linear input polarization, nothing happens.

A half wave plate can be thought of simply as two quarter wave plates in series. So consider linearly polarized light at θ = 45° incident upon the first of two quarter wave plates. The output of the first quarter wave plate is circularly polarized. Passing through the second quarter wave plate, the light becomes linearly polarized again, but at an angle of 90° relative to the original polarization direction. (Rays are reversible.) This is a special case, easy to visualize, which shows that the half wave plate rotates linear polarized light through 2θ. In general, when the input polarization is at an angle θ relative to the fast axis of a half wave plate, the output polarization is rotated through 2θ relative to the input polarization.

Linear Polarizer

A linear polarizer optimized for infrared wavelengths is available. It is mounted in a rotary mount labeled “Melles Griot,” the manufacturer. The easy axis of the polarizer is marked with two small white tick marks on the inner housing of the polarizer. Use it to verify the direction and type of polarization of the laser beam and the action of the waveplates. The polarizer will extinguish linearly polarized light (at 90°) and appear isotropic to circularly polarized light.

Linearly polarized light can be thought of as a superposition of right- and left-circularly polarized light of equal intensities.

Jones Vectors and Matrices are a convenient way of expressing the actions of wave plates on polarized light. See http://scienceworld.wolfram.com/physics/JonesVector.html

Polarizing Cubes

Four cubes, three of which are sensitive to polarization, are used as beamsplitters. The cubes are composed of two right-angle prisms cemented together. For the polarizing cubes, the interface between the prisms reflects vertically-polarized light at 90° and transmits horizontally-polarized light.

The first cube splits the beam between the low-pressure rubidium cell (for the saturated absorption spectroscopy) and the magnetic shield (for dark resonance and slow light). A half-wave plate upstream of this cube can be used to rotate the polarization of the input light. Thus the intensity of the reflected and transmitted beams can be varied.

The second, smaller cube is not sensitive to polarization. It splits off a beam used as a reference in the slow light measurement. A third cube selects the component of the reference beam which has been rotated by the Pockels cell (more below).

The fourth cube, installed downstream of the magnetic shield, is used as a polarization analyzer. A quarter wave plate upstream of it but downstream of the magnetic shield re-linearizes circularly polarized light. Thus in conjunction with the quarter wave plate and two photodetectors, this cube acts as an analyzer to resolve the right- and left-circular components of the beam.

Pockels Cell

The Pockels Cell (Conoptics 350-80LA or Lasermetrics 3079-4), made of a birefringent material, acts as a voltage-variable wave plate. The voltage required for half-wave retardation is several hundred volts. A dc amplifier (Lasermetrics AF3) provides a $\pm$650V output, which can be a combination of dc and ac signals. A gaussian pulse from the Stanford Research Systems DS345 function generator can be used for input to the AF3. The input signal should be 1V peak-to-peak maximum. Start with the gain control set to minimum and the dc offset switch set to its center position (off). To test the functionality of the Pockels cell, monitor horizontal and vertical polarization components of the beam using the polarization analyzer. Begin by switching on the positive dc offset and slowly increasing its value. You should see one polarization component increase and the other decrease. Next connect the input signal, and slowly increase the gain. The polarization analyzer should detect anticorrelated modulations of the polarization components, synchronized with the input signal.

Photodetectors

Two types of silicon photodetectors are in use: Thorlabs PDA55 and Thorlabs DET110. The PDA55s require a dc input, and incorporate a variable-gain transimpedance amplifier. The DET110s are battery operated; please switch them off at the end of the lab period. Since the output is a current, they require a terminating resistor (10 kΩ recommended).

Magnetic Shield, Oven and Solenoid

A schematic end-view of the magnetic shield assembly is shown at right.

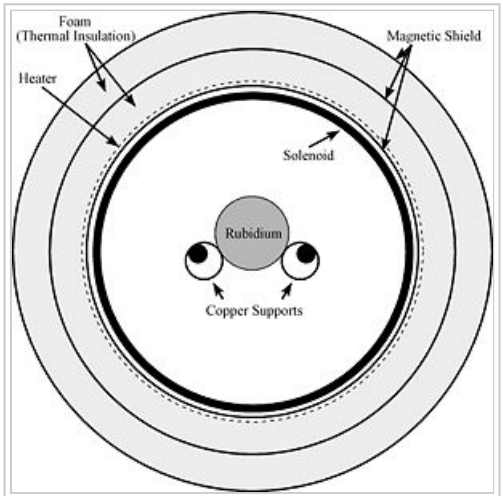

Magnetic shield assembly

Magnetic Shield

A three-layer cylindrical mu-metal shield screens the rubidium cell from the earth's magnetic field as well as stray fields generated in the laboratory. The cylindrical portions of the shield are held in place by sheets of foam, which also act as thermal insulation. The shields can be disassembled to change the rubidium cell or for viewing. The easiest way to do this is by removing the mu-metal caps from the downstream end of the apparatus. The rubber grommets that hold the copper supports in place are cut in half on the downstream end to facilitate disassembly.

Oven

A heater is wound around the inner cylinder. The heater is designed in a non-inductive manner to minimize magnetic disturbances. Even so, you may get stronger signals by turning off the heater once the oven is heated up to the desired temperature. The heater has a resistance of about 92Ω. Two resistors (6Ω total) are wired in series with the heater to protect the power supply in case of an accidental short circuit. A Harrison 6200A regulated dc power supply provides power to the heater. The time constant for heating is on the order of hours, so it's best to turn the oven on in the morning before lab. At 28 V, (300 mA), the oven reaches a temperature of about 60°C which is sufficient to observe a robust dark resonance, and to detect a slow-light signal.

Solenoid

The solenoid is wound on a slotted aluminum frame. It consists of two layers of #28 high temperature magnet wire. The bottom layer has 544 turns and the top layer 518 turns. The solenoid length is 8 inches, and the inner diameter is 107 mm. The resistance of the solenoid is 78Ω, so it can be driven directly by one of the function generators. The strength of the magnetic field is 0.82 Gauss/Volt.

NOTES

1. ↑ For a general, classical treatment of resonance phenomena, see, e.g., D.J. Griffiths, *Introduction to Electrodynamics*, Prentice Hall (2002), page 398.
2. ↑ An introduction to the modern treatment of two-level systems can be found in P. Meystre and M. Sargent, *Introduction to Quantum Optics*, Chapters 4 and 5. For theoretical discussion of the three level systems and dark resonances see M.O. Scully and M.S. Zubairy, *Quantum Optics*, Chapter 7.
3. ↑ In fact, "perfect isolation" implies also an isolation from vacuum fluctuations of the electromagnatic field. As you can imagine, achieving such isolation is a very non-trivial task. Nevertheless, ideas of this kind are now increasingly realistic, and are being explored in the field of cavity quantum electrodynamics.
4. ↑ Since the dark-state phenomenon involves coherence between the ground states $|g\rangle$ and $|g'\rangle$, the ultimate linewidth γ_0 of a dark-resonance can be orders of magnitude smaller than both the Doppler width and the spontaneous emission rate of the electronic excited state.
5. ↑ For detailed discussion of various concepts and techniques in nonlinear optics, see R.W. Boyd, *Nonlinear Optics*, Academic Press (2002).
6. ↑ A rather complete introduction to early work on dark-resonances: E. Arimondo, *Progress in Optics*, (ed. E. Wolf), Vol. 35, 259-354, North Holland, Amsterdam (1996).

REFERENCES

For a nice introduction and discussion of Rb spectra, see J. Vanier and C. Audoin, *The quantum physics of atomic frequency standards*, Adam Hilger (1989).

A good general reference on modern spectroscopy is W. Demtroder, *Laser Spectroscopy*, Springer (1996).

D.W. Preston, "Doppler-free saturated spectroscopy: laser spectroscopy," American Journal of Physics **64** (11), 1432 (1996) and references

therein.

An accessible review on Electromagnetically Induced Transparency: S.E. Harris, Physics Today **50**, 36 (1997).

An account of "slow light" experiments in Bose-Einstein condensates: L. Hau, Scientific American (2001).

General review on nonlinear magneto-optic phenomena, including the nonlinear Faraday effect: D. Budker et al., Review of Modern Physics **74**, 1153 (2002).

An overview of some modern applications of dark-resonances in physics: M.D. Lukin, Review of Modern Physics **75**, 457 (2003).

A nonlinear optics experiment at UC Berkeley: D. Budker, D.J. Orlando, V. Yashchuk, "Nonlinear laser spectroscopy and magneto-optics," American Journal of Physics, **67**, 584 (1999).

Contains one simple article on Doppler-free resonance: F.T. Arecchi, F. Strumia, H. Walther and North Atlantic Treaty Organization (Scientific Affairs Division), *Advances in Laser Spectroscopy*, Plenum Press, New York, (1983). NATO Advanced Study Institute on Advances in Laser Spectroscopy (1981: San Miniato, Italy).

Further Reading:

D.A. Steck. Rubidium 87 D Line Data (http://www.fas.harvard.edu/~phys191r/References/a4/rb87.pdf) .

D. Budker. "Nonlinear laser spectroscopy and magneto-optics (http://www.fas.harvard.edu/~phys191r/References/a9/Budker_AJP.pdf) ," American Journal of Physics 67, 584 (1999).

D. Budker, "Resonant nonlinear magneto-optical effects in atoms (http://www.fas.harvard.edu/~phys191r/References/a9/Budker_RMP.pdf) ," Review of Modern Physics, (4Jun2002).

M. S. Shahriar, "Dark-state-based three-element vector model for the stimulated Raman interaction (http://www.fas.harvard.edu/~phys191r/References/a9/Shariar1997.pdf) ," Physical Review A 55, 3, 2272 (1997).

P. R. Hemmer, M. G. Prentiss, "Coupled-pendulum model of the stimulated resonance Raman effect (http://www.fas.harvard.edu/~phys191r/References/a9/coupledpendulum.pdf) ," J. Opt. Soc. Am. B 5, 8, 1613 (1988).

R. Walsworth, S. Yelin, and M. Lukin, "The Story Behind 'Stopped Light' (http://www.fas.harvard.edu/~phys191r/References/a9/OPN_stopped_light.pdf) ," Optics and Photonics News, May 2002, 51-54,76.

J.P. van der Ziel, P.S. Pershan, L.D. Malmstrom, "Optically-induced magnetization resulting from the inverse Faraday effect (http://www.fas.harvard.edu/~phys191r/References/a9/Pershan1965.pdf) ," Phys. Rev. Lett., 15, 190 (1965).

BENCH NOTES

- Wavetek 188 Function Generator (http://www.fas.harvard.edu/~phys191r/Bench_Notes/A9/Wavetek188.pdf)
- Stanford Research Systems DS345 Function Generator (http://www.fas.harvard.edu/~phys191r/Bench_Notes/A9/DS345m.pdf)
- Hewlett Packard 8111A Function Generator (http://www.fas.harvard.edu/~phys191r/Bench_Notes/A9/hp8111a.pdf)
- Thorlabs DET110 Photodiode (http://www.fas.harvard.edu/~phys191r/Bench_Notes/A9/det110.pdf)
- Thorlabs PDA55 Photodiode (http://www.fas.harvard.edu/~phys191r/Bench_Notes/A9/PDA55.pdf)
- Uvex DVO Laser Eyewear (http://www.fas.harvard.edu/~phys191r/Bench_Notes/A9/goggles.pdf)
- Newport RPR-36-8 Optical Tabletop (http://www.fas.harvard.edu/~phys191r/Bench_Notes/A9/rpr.pdf)
- Newport PL-2000 Pneumatic Legs (http://www.fas.harvard.edu/~phys191r/Bench_Notes/A9/pl2000.pdf)
- CVI Waveplates (http://www.fas.harvard.edu/~phys191r/Bench_Notes/A9/QWPO.pdf)
- CVI Polarizing Beamsplitter Cubes (http://www.fas.harvard.edu/~phys191r/Bench_Notes/A9/PBS.pdf)
- Conoptics 350-80LA Pockels Cell (http://www.fas.harvard.edu/~phys191r/Bench_Notes/A9/conoptics.pdf)
- New Focus Laser Specifications (http://www.fas.harvard.edu/~phys191r/Bench_Notes/A9/vortex6017.pdf)
- New Focus Laser User's Guide (http://www.fas.harvard.edu/~phys191r/Bench_Notes/A9/vortex6000.pdf)
- Lasermetrics 3079-4 Electro-Optic Light Modulator (Pockels Cell) (http://www.fas.harvard.edu/~phys191r/Bench_Notes/A9/3079.pdf)
- Lasermetrics 3079-4 User's Guide (http://www.fas.harvard.edu/~phys191r/Bench_Notes/A9/3079user.pdf)
- Lasermetrics AF3 High-Voltage Amplifier (http://www.fas.harvard.edu/~phys191r/Bench_Notes/A9/AF3.pdf)
- Lasermetrics AF3 User's Guide (http://www.fas.harvard.edu/~phys191r/Bench_Notes/A9/AF3user.pdf)
- Electro-Optic Devices in Review (http://www.fas.harvard.edu/~phys191r/Bench_Notes/A9/EOreview.pdf)
- Series Resistor Box Schematic (http://www.fas.harvard.edu/~phys191r/Bench_Notes/A9/series_resistor_box.pdf)
- Slow Light Apparatus Notes (Mason Klein) (http://www.fas.harvard.edu/~phys191r/Bench_Notes/A9/mason_notes.pdf)
- Rb Maser Notes (number density etc.) (http://www.fas.harvard.edu/~phys191r/Bench_Notes/A9/rb_maser.pdf)

- Mathematica Polarization calculator (P. Pershan 10/09) (http://www.fas.harvard.edu/~phys191r/Bench_Notes/A9/Polarization2.nb)

Links

- Rubidium Energy Level Diagrams (David Phillips) (http://cfa-www.harvard.edu/%7Edphil/work/rbmaser/index.html)
- Jones Vectors and Matrices (http://scienceworld.wolfram.com/physics/JonesVector.html)
- Lecture Notes on Selection Rules (David Ritchie, University of Cambridge) (http://www.fas.harvard.edu/~phys191r/Bench_Notes/A9/selection_rules.pdf)

APPENDIX: Alternate Perspective on Dark Resonance

author: P.S. Pershan (2004)

An alternative way to look at the Dark Resonance Phenomena when the laser frequency is away from the absorption resonance is to start from the energy density of an electromagnetic field in a material of dielectric constant ϵ. For example in the presence of an external electric field $\vec{E}$ the energy of a polarizable atom is reduced by

Eq. 1 $\delta U = -\vec{E} \cdot \delta\vec{p} = -\alpha\delta\left(\frac{E^2}{2}\right)$

where α, the atomic polarizability, can be expressed quantum mechanically as

Eq. 2 $\alpha \sim \sum_{e,g} \omega_{ji} \frac{|\langle g|r|e\rangle|^2}{\omega_{eg}^2 - \omega^2}$.

In this expression 'g' refers to the ground state and 'e' to the excited state, ω is the frequency of the field and $\omega_{eg} = (E_e - E_g)/\hbar$ corresponds to the excitation energy between 'g' and 'e'. Note that $\alpha(\omega)$ is a function of frequency and this approximation is only valid when $|\omega_{eg} - \omega| \gg$ *Width of the resonance*. As $\omega_{eg} - \omega \to 0$, α becomes complex and this gives rise to absorption. Although the formulae become more complicated the physics is essentially the same as for the non-resonant case.

Consider only the $m = \pm 1$ components of an $L = 1$ ground state. Their wave functions have the form

Eq. 3 $\psi_{\pm 1}(\vec{r}) = \frac{x \pm iy}{r} f(r)$.

In the absence of an external magnetic field these are degenerate and the ground states can be formed by any linear combination. Say for example

Eq. 4 $\psi_x = \frac{\psi_+ + \psi_-}{\sqrt{2}} = \sqrt{2}\frac{x}{r} f(r) \quad \text{and} \quad \psi_y = \frac{+\psi_+ - \psi_-}{i\sqrt{2}} = \sqrt{2}\frac{y}{r} f(r)$.

If the electric field is polarized along the x-direction the linear combination in Eq. 4 is the natural one to choose since in this form the Hamiltonian has the form

Eq. 5 $\begin{bmatrix} U_{xx} & U_{xy} \\ U_{yx} & U_{yy} \end{bmatrix} = \begin{bmatrix} -\alpha E^2/2 & 0 \\ 0 & 0 \end{bmatrix}$.

This non-linear term lifts the degeneracy of the ground state in a particular manner.

If, instead of an electric field there was an externally applied magnetic field applied along the z-axis the Zeeman splitting would lift the degeneracy as

Eq. 6 $\begin{bmatrix} U_{++} & U_{+-} \\ U_{-+} & U_{--} \end{bmatrix} = \begin{bmatrix} -\mu H & 0 \\ 0 & \mu H \end{bmatrix}$.

Making use of the unitary transformation

Eq. 7 $$\begin{bmatrix} \psi_x \\ \psi_y \end{bmatrix} = \frac{1}{\sqrt{2}} \begin{bmatrix} 1 & 1 \\ -i & i \end{bmatrix} \begin{bmatrix} \psi_+ \\ \psi_- \end{bmatrix} \quad \text{and} \quad \begin{bmatrix} \psi_+ \\ \psi_- \end{bmatrix} = \frac{1}{\sqrt{2}} \begin{bmatrix} 1 & i \\ 1 & -i \end{bmatrix} \begin{bmatrix} \psi_x \\ \psi_y \end{bmatrix}$$

the Zeeman form can be expressed as

Eq. 8 $$\begin{bmatrix} U_{xx}^Z & U_{xy}^Z \\ U_{yx}^Z & U_{yy}^Z \end{bmatrix} = \frac{1}{2} \begin{bmatrix} 1 & 1 \\ -i & i \end{bmatrix} \begin{bmatrix} -\mu H & 0 \\ 0 & \mu H \end{bmatrix} \begin{bmatrix} 1 & i \\ 1 & -i \end{bmatrix} = \mu H \begin{bmatrix} 0 & -i \\ i & 0 \end{bmatrix}.$$

Combining Eq. 5 and Eq. 8 for the case when there is both an optical E-field and a static H-field the ground state Hamiltonian for $m = \pm 1$ has the form

Eq. 9 $$\begin{bmatrix} U_{xx}^{EH} & U_{xy}^{EH} \\ U_{yx}^{EH} & U_{yy}^{EH} \end{bmatrix} = \begin{bmatrix} -\alpha E^2/2 & -i\mu H \\ i\mu H & 0 \end{bmatrix}.$$

The eigenvalues for this Hamiltonian have the form

Eq. 10 $$U_{eigen} = -\frac{\alpha E^2}{4} \pm \left\{ \left(\frac{\alpha E^2}{4} \right)^2 + \mu^2 H^2 \right\}^{1/2}$$

with eigenvectors of the form

Eq. 11 $$\begin{aligned} \psi_1 &\propto i \left[\frac{\alpha E^2}{4} + \left\{ \left(\frac{\alpha E^2}{4} \right)^2 + \mu^2 H^2 \right\}^{1/2} \right] \psi_x + \mu H \psi_y \\ \psi_2 &\propto i \left[-\frac{\alpha E^2}{4} + \left\{ \left(\frac{\alpha E^2}{4} \right)^2 + \mu^2 H^2 \right\}^{1/2} \right] \psi_x + \mu H \psi_y \end{aligned}$$

Although these equations are derived for the non-resonant case, the physics of the absorption case is essentially described by these wavefunctions. In view of the fact that the E-field is along the x-direction the transition matrix that is responsible for optical pumping only involves ψ_x. From these expressions one can see that if H=0 the optical absorption is only from the state ψ_1, which for H=0 is just ψ_x. For H=0 the pumping process will transfer all the atoms to either the or ψ_2 state, which is just ψ_y when H=0. On the other hand, with finite H there is absorption from both of the eigenstates described by Eq. 11 and the condition for a dark state is no longer satisfied. In this case the matrix elements lead to elliptically polarized optical polarization and this in turn gives rise to optical rotation.

Retrieved from "https://coursewikis.fas.harvard.edu/phys191r/A-9_Nonlinear_Optics"